GLOBAL ACADEMIC RESEARCH INSTITUTE

COLOMBO, SRI LANKA

GARI International Journal of Multidisciplinary Research

ISSN 2659-2193

Volume: 09 | Issue: 02

On 30th June 2023

http://www.research.lk

Author: Dinuka Fernando, Dr. Mathivathani Kandiah

School of Science, BMS, Sri Lanka

GARI Publisher | Microbiology | Volume: 09 | Issue: 02

Article ID: IN/GARI/JOU/2022/158 | Pages: 116-137 (21)

ISSN 2659-2193 | Edit: GARI Editorial Team

Received: 04.04.2023 | Publish: 30.06.2023

ECO FRIENDLY SYNTHESIS OF SILVER NANOPARTICLES USING FIVE VARIETIES OF ANNONACEAE LEAF EXTRACT AND ASSESSING THEIR POTENTIAL ANTIOXIDANT, PHOTOCATALYTIC, AND ANTIBACTERIAL EFFECTS

Dinuka Fernando, Dr. Mathivathani Kandiah

School of Science, BMS, Sri Lanka

ABSTRACT

The development of eco-friendly, and sustainable methods to synthesize silver nanoparticles (AgNPs) is a rapidly developing field in nanotechnology. In this study five varieties of Annonaceae leaves were used to synthesis AgNPs to investigate the antioxidant, photocatalytic and antibacterial properties. The water extract was prepared by mixing 2g of sample with 50mL of water and was heated at 95°C for 20minutes. The phytochemical analysis uncovered the presence of phytochemical compounds. 1mL of water extract was mixed with 9mL of 1mM AgNO3 solution and was optimized at different temperatures and time intervals. The formation of AgNPs was observed by a colour change and was confirmed by the UV-Vis spectroscopy which displayed a plasmon resonance peak between 420-440nm. The size and shape of Annona squamosa red AgNPs were investigated by the scanning-electron microscope, and it was spherical in shape and with size of 40nm. The antioxidant properties were analysed by Total Phenolic Content, Total Antioxidant Content, and Total Flavonoid Content. High levels of antioxidants were observed in the AgNPs than water extracts. The photocatalytic activity of Annona squamosa red AgNPs was analysed by Methyl Red for 267 ppm, and 4000 ppm and under UV light and sunlight with and without the presence of NaBH4 catalyst. The degradation of methyl red was partially achieved without NaBH4 in 75 minutes. The AgNPs showed a significant antibacterial activity against Escherichia coli and Staphylococcus aureus. The findings confirmed that the green synthesized AgNPs can be used in a variety of medical and environmental applications.

Key words: silver nanoparticles, Annonaceae leaves, antioxidant, photocatalyst, antimicrobial.

INTRODUCTION

Nanotechnology is a broad area of research offering a wide range of unique applications in agriculture, health care, medical sciences, and food industries (Hemlata et al., 2020). Nanotechnology is the portrayal, manufacture, manipulation, and application of structures by controlling shape and size at a nanoscale (Hood,2004). The synthesis of nanoparticles is one of most modern areas of research, where particles with at least one dimension between 1 and 100 nm are synthesized and stabilized using nanotechnology (Baig, Kammakakam & Falath, 2021). The two primary methods for creating nanoparticles are top-down and bottom-up approaches (Figure 1). The top-down approach is initialized by bulk counterpart that leaks out slowly leading

to the synthesis of nanoparticles whereas the bottom-up approach involves assembly of atoms, molecules, and clusters to produce nanoparticles (Dhand et al., 2015).

The concept of green synthesis has been widely researched and developed to counter the current environmental crisis. While chemical synthesis is more toxic and costly, green synthesis is an environmentally friendly approach as it avoids producing toxic products. Bacteria is also an excellent choice to synthesize nanoparticles as it can reduce heavy metal ions. Nevertheless, there are difficulties with this approach, including culture contamination, drawn-out procedures, and limited control over nanoparticle size (Mustapha et al., 2022).

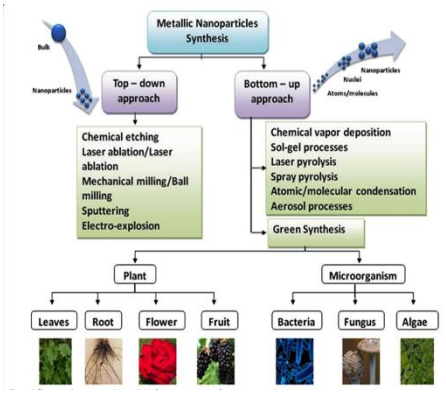

Figure 1 -Different approaches to synthesize nanoparticles (Singh et al., 2018)

Although some noble elements have shown excellent production of nanoparticles, the production of non-toxic metal nanoparticles has been a significant issue. Silver nanoparticles (AgNPs) display significant properties such as surface plasmon resonance (SPR), chemical stability, high conductivity, anti-bacterial and anti-viral properties. AgNPs does not have any toxic effects on human cells but has inhibitory effects on bacteria, viruses, and micro-organisms (Mustapha et al., 2022).

The most crucial phase of nanoparticle synthesis is creating a method that regulates the size, shape, stability, and physicochemical properties as they are highly influenced by factors such as temperature, pH, and reducing agents (Zhang et al., 2016). Silver ion (Ag+) undergoes a reduction reaction, changing from a positive valence to a zero-valent state (Ag0), followed by nucleation and growth (Figure 2). As a result, colloidal AgNPs are produced by coarse aggregation into oligomeric clusters (Lee & Jun 2019).

Different phytochemicals that contain hydroxyl and carboxyl functional groups such as phenols, act as a capping, and a reducing reagent therefore stabilizing the conversion of Ag+1 ions to stable Ag0 (Melkamu & Bitew, 2021).

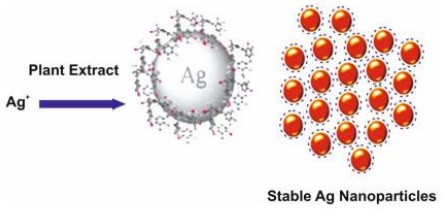

Figure 2 - Formation of Silver Nanoparticles (Selvaraj et al., 2019)

In this study five varieties of Annona leaves from the Annonaceae family were used to synthesize AgNPs. Annona plants have been receiving a large amount of attention due to the presence of anti-cancer, anti-inflammatory, antioxidant, antiparasitic, and insecticidal properties (Coria-Téllez et al., 2018). Due to commercial popularity of Annona fruits, the leaves are not widely utilized to gain the maximum health benefits they offer. Thus, leaves are considered a waste product although certain research has proven immense health benefits if utilized efficiently.

The word ‘antioxidant’ has gained a large amount of public attention as they play a vital role in protecting the human body against free radicals by working as free radical scavengers thus delaying and preventing oxidation (Nguyen et al., 2020). The generation of free radicals and reactive oxygen species (ROS) during metabolism will give rise to excessive oxidative stress which causes damage to macromolecules (Figure 3) and leads to the development of degenerative diseases. (Hano & Abbasi, 2021).

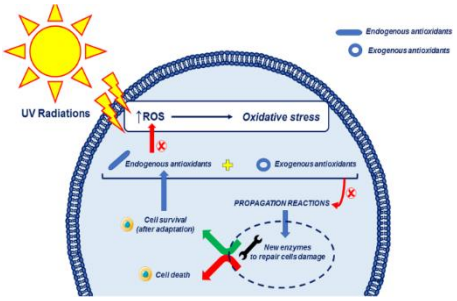

Figure 3 - Oxidative production pathways (Lorigo & Cairrao, 2019)

ROS such as superoxide (•O2−), hydroxyl radical (•OH), singlet oxygen (1/2 O2), and hydrogen peroxide (H2O2) are beneficial in low concentrations assisting immune reactions against pathogens and cell maturation but harmful in high concentrations leading to mutations, and carcinogenesis (Valko et al., 2007). Due to the low cost and excellent efficacy, synthetic antioxidants like butylated hydroxyl anisole have been produced commercially. Despite the widespread use of synthetic antioxidants, safety concerns have been raised due to skin allergies, gastrointestinal problems, and increased risk of cancer. As a result, there has been a rising trend in developing plant-based antioxidants in place of synthetic ones (Lourenço, Moldão-Martins & Alves, 2019).

A severe issue to public health and a hazard to human life is the ongoing evolution of bacterial strains resistant to the present antibiotics. The effect of plant extracts on bacteria has been widely studied as a need to develop antibacterial agents as an alternative natural strategy. The antimicrobial activity varies according to the nanoparticle size, shape, and inherent constituents of the structure thus the cell membrane can be easily penetrated and cause damage to cellular matter in a gram-negative bacterium Escherichia coli and gram-positive bacterium Staphylococcus aureus (Fanoro & Oluwafemi, 2020).

Synthetic organic colorants that contain one or more chromophoric azo groups (-N=N) are known as azo dyes (Figure 4). Various number of azo dyes are in demand due to the commercial use of dyes in industries such as textiles, printing, and cosmetics. Due to the toxic and non-degradable nature, the production and disposal of organic dyes are a significant issue faced at present (Vatandoostarani et al., 2017). Lately nanoparticles have been found to have photocatalytic properties to degrade organic dyes under visible light which will give rise to the remediation of the environment (Roy, Sarkar, & Ghosh, 2015).

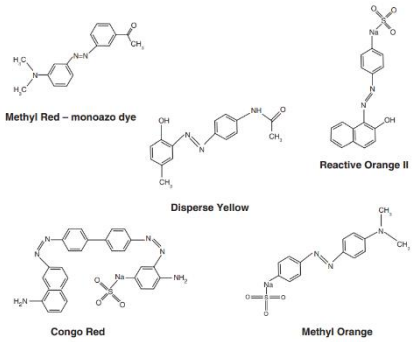

Figure 4 - Azo dyes (Sreedharan & Bhaskara Rao, 2019)

The study focused on the green synthesis AgNPs from five varieties of water leaf extracts from the Annona plant, to determine and evaluate anti-bacterial properties, antioxidant properties, and photocatalytic activity. By utilizing the well diffusion method, the antimicrobial activity will be assessed using gram-negative bacterium Escherichia coli (E.coli) and gram-positive bacterium Staphylococcus aureus (S.aureus). Total flavonoid content (TFC), total phenolic content (TPC), total antioxidant content (TAC), 2,2-Diphenyl-1-picrylhydrazyl (DPPH) Scavenging Activity and median inhibition concentration (IC50) assays will be performed to evaluate the antioxidant activity. The photocatalytic activity will be evaluated by the degradation of methyl red (MR) dye. The size and shape will be analyzed by scanning electron microscope (SEM). As a result of this study Annona leaves could be successfully used as a pharmaceutical agent due to antioxidant, photocatalytic and antibacterial properties.

MATERIALS

Chemical Reagents

Aluminium chloride (AlCl3) (CAS-7446-70-0), ammonium hydroxide (NH4OH), ammonium molybdate ([NH4]6 Mo7O24.4H2O), chloroform (CH3Cl) (CAS-67-66-3), copper sulphate (CuSO4) (CAS-7758-98-7), 2,2-diphenyl-1-picrylhydrazyl (DPPH) (CAS-1898-66-4), ethanol (C2H5OH) (CAS- 64-17-5), ferric chloride (FeCl3) (CAS-7705-08-0) , Folin–Ciocalteu phenol reagent, methanol (CH3OH) (CAS-67- 56-1), hydrochloric acid (HCl) (CAS-7647-01-01-0), McFarland solution, methylene red (C15H15N3O2) (493-52-7), Molisch's reagent, Mueller-Hinton agar powder, nutrient agar powder, saline, silver nitrate (AgNO3) (CAS-7761-88-8), sodium borohydride(NaBH4), sodium carbonate (Na2CO3) (CAS-497-19-8), sodium hydroxide (NaOH) (CAS 1310-73-2), sodium nitrate (NaNO3) (CAS 7631-99-4), sodium sulphate (Na2SO4) (CAS 7757-82-6), sulphuric acid (H2SO4) (CAS-7664-93-9).

Apparatus

Hot-air oven (meditry DHA-9053A), incubator, analytical balance, spectrophotometer (JENWAY 6305), roller mixer, micropipettes, refrigerator, fume hood (Biobased FH1000), and autoclave.

Glassware and Miscellaneous

Conical flask, measuring cylinder, filter funnel, spatulas, test tubes, cuvette, volumetric flask, Petri dishes, beakers, cotton swabs, watch glass, filter paper, falcon tubes, and Whatman filter papers No.1.

METHODOLOGY

All the methodologies in the research were performed according to the safety regulations provided by the bioCOSHH and COSHH forms respectively.

Sample collection

Fresh leaves of five varieties of Annona plants (Figure 5) were gathered from Athurugiriya, Sri Lanka.

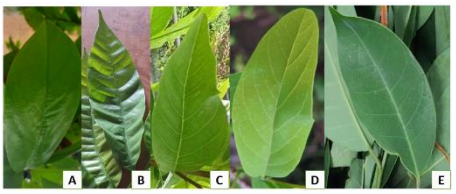

Figure 5 - A. Annona muricata, B. Annona reticulata, C. Annona squamosa green, D. Annona squamosa red, E. Annona glabra

Table 1 - Code name for the leaves

Sample	Code name	
	Water Extract	Nano particles
Annona muricata	*A.muricata*	*A.muricata*-AgNPs
Annona reticulata	*A.reticulata*	*A.reticulata*-AgNPs
Annona squamosa green	*A.squamosa* green	*A.squamosa* green-AgNPs
Annona squamosa red	*A.squamosa* red	*A.squamosa* red-AgNPs
Annona glabra	*A.glabra*	*A.glabra*-AgNPs

Sample preparation

The Annona leaves were washed with distilled water to remove contaminations, shade dried for seven days and grounded. For extract preparation, 2g of grounded leaves was mixed with 50mL of distilled water in a beaker wrapped in foil and boiled at 95°C for 20 minutes. The prepared leaf extraction was filtered using Whatman No.1 filter paper to obtain a clear extract and put in storage at 4°C for further experiments. (Jagtap & Bapat, 2012).

Phytochemical analysis

By using the aqueous leaf extracts the preliminary phytochemical analysis was performed (Table 2).

Table 2 - Methodology of phytochemical analysis

Phytochemical	Methodology	Expected Results
Carbohydrate	0.5mL of extract was treated with few drops of Molisch's reagent and few drops of concentrated H_2SO_4 were added.	Formation of red ring.
Amino acid	0.5mL of extract was treated with a drop of ninhydrin solution.	Purple color.
Proteins	0.5mL of extract was treated with few drops of Millon's reagent.	White precipitate.
Saponins	0.5mL of extract was treated with 1mL of distilled water and was shaken for 5 minutes.	Formation of white foam.
Tannins	0.5mL of extract was treated with 1mL of 5% $FeCl_2$	Green-black solution.
Quinones	0.5mL of extract was treated with 0.5mL of H_2SO_4	Red color.
Terpenoids	0.5mL of extract was treated with 2mL of chloroform and 2mL of H_2SO_4	Brown color solution.
Steroids	0.5mL of extract was treated with 0.5mL of chloroform and few drops of H_2SO_4	Brown color ring.
Phlobatannins	0.5mL of extract was treated with 0.5mL of HCL and was heated.	Red color solution with precipitate.

Green synthesis of silver nanoparticles

1 mM of AgNO3 solution was made by dissolving 0.0169g of AgNO3 in 100mL of distilled water. 1mL of each plant extract was mixed with 9mL of AgNO3 of the prepared solution. The samples were optimized at 90°C, 60°C, and 45°C temperature, for time periods of 15, 30, and 60 minutes. The absorbance was monitored in the range of 320 to 500 nm by using a UV-spectrophotometer for each optimization using a blank.

Preparation of diluted samples

1:15 sample dilution was conducted for both extract and AgNPs samples. 1mL of extract was diluted with 14mL of distilled water for each sample. Diluted samples were stored at 4°C and different assays were carried out for both water extract and AgNPs.

Determination of Total Flavonoid Content

Based on the AlCl3 colorimetric technique, the TFC assay was performed for all samples. (Kandiah & Perera, 2018). 0.5mL of sample was mixed with 0.5mL of 2% AlCl3, the tubes were shaken and left for 15 minutes. Using distilled water as a blank the intensity of color was measured at 415 nm in triplicates. The findings were demonstrated in µg Quercetin equivalents per 100g (µg QE/100 g).

Determination of Total Phenolic Content

According to the Folin Ciocalteu (FC) method, 1mL of 10% FC reagent was mixed with 1mL of sample. Next, 1mL of Na2CO3 was added and the sample was shaken. After 30 minutes of incubation in the dark at room temperature the intensity was measured at 765 nm in triplicates with a distilled water blank. The TPC was expressed in mg of gallic acid equivalents per gram of sample (mg GAE/g) (Nguyen et al., 2020).

Determination of Total Antioxidant Content

TAC for samples was carried out by the phosphomolybdenum assay. Equivalent volumes of 28 mM Na2SO4 and 4 mM ammonium molybdate and 0.6 M H2SO4 (1:1:1) were mixed to obtain the phosphomolybdenum regent. 1mL of regent was mixed with the samples and placed in a water bath at 90°C for 90 minutes. After cooling the absorbance was measured at 695 nm against a water blank. The experiment was conducted in triplicates and the values were expressed in ascorbic acid equivalence (mg AAE / 100 g) (Kumar & Jain, 2015).

Determination of DPPH Scavenging Activity

The sample was combined with 2 mL of a 0.004% DPPH solution in ethanol. The mixture was kept in the dark and incubated at room temperature for 30 minutes. Absorbance was measured at 517 nm in triplicates using methanol as a blank. The radical scavenging activity was calculated according to equation 1 given below (Kandiah & Perera, 2018).

$$Inhibition\ (\%) = Control - \frac{Sample}{Control} \times 100$$

Equation 1

Determination of Median Inhibition Concentration

1mL of series of six concentrations (100%, 80%, 60%, 40%, 20% and 10%) of the sample was prepared by distilled water and mixed with 2mL of 0.004% DPPH. The samples were placed in the dark for 30 minutes. Absorbance was measured at 734 nm using methanol as a blank (Kandiah & Perera, 2018).

Antibacterial Assay

The Muller-Hinton agar well diffusion assay was performed under aseptic

conditions to evaluate the antibacterial activity against E.coli and S.aureus. The bacterial inoculum was consistently distributed on the agar using a sterile cotton swab and three wells were created using a sterile tip and the petri plates were labelled (Figure 6). 1mL of the sample was introduced to each well, 1mL of saline was loaded to the negative control. Gentamycin was impregnated in the positive control. The petri dishes were incubated at 37°C overnight and the diameter of the zone of inhibition (ZOI) was measured in centimeters (Kandiah & Perera, 2018).

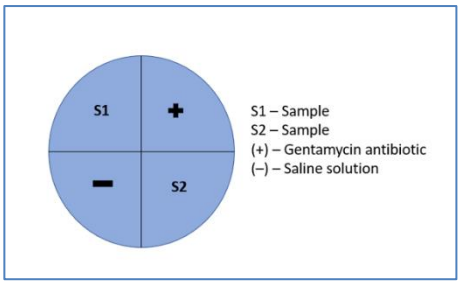

Figure 6 - Labeling of petri plates

Photocatalytic degradation of methyl red dye

A.squamosa red-AgNPs were chosen to observe photocatalytic degradation under different conditions (Kandiah & Perera, 2018).

Sunlight

50mL of the 2 mM MR solution was prepared, and 0.5mL of the 267-ppm sample was introduced to the MR solution. The sample was left under the sunlight. Absorbance was measured from 300 to 600 nm every 30 minutes for 120 minutes using distilled water as a blank. The procedure was repeated at 3000 ppm.

Sunlight with NaBH4

50mL of the 2 mM MR solution was prepared, and 0.5mL of 0.2 M of NaBH4 was added to the solution. 0.5mL of the 267-ppm sample was introduced to the MR solution. The sample was kept under the sunlight. Absorbance was measured from 300 to 600 nm every 30 minutes for 120 minutes using distilled water as a blank. The procedure was repeated at 3000 ppm.

Nanoparticle Composition, Size distribution, and Statistical Analysis

Morphological findings were analyzed by SEM analysis. After a 15-minute centrifugation at 5000 rpm with A.squamosa red-AgNPs the sample was incubated overnight at 50°C. The sample was analyzed by the Scanning Electron Microscope at Sri Lankan Institute of Nanotechnology, Homagama, Sri Lanka using the Hitachi SU6600 SEM.

In order to establish a statistical difference One-way ANOVA was generated using Microsoft® Excel 2016 software and the correlation graphs were created using IBM SPSS Statistics 23 software.

RESULTS

Phytochemical Analysis

Table 3 - Phytochemical Analysis

Phytochemical test	*Annona muricata*	*Annona reticulata*	*Annona squamosa Green*	*Annona squamosa Red*	*Annona Glabra*	Positive Result
Carbohydrate	✓	✓	✓	✓	✓	Purple ring.
Amino acid	✓	✓	✓	✓	✓	Dark purple solution
Saponins	✓	✓	✓	✓	✓	Formation of Form
Tannins	✓	✓	✓	✓	✓	Green black solution.
Proteins	✗	✓	✓	✓	✗	White precipitate
Steroids	✗	✓	✓	✓	✓	Brown ring
Terpenoids	✗	✓	✓	✓	✓	Brown ring
Phlobatannins	✓	✓	✓	✓	✓	Red color

Phytochemical analysis was done for all five water extracts.

Synthesis of silver nanoparticles

A change in colour from yellow to red was observed after 24 hours indicating the formation of AgNPs for A.muricata, A.squamosa green and A.squamosa red.

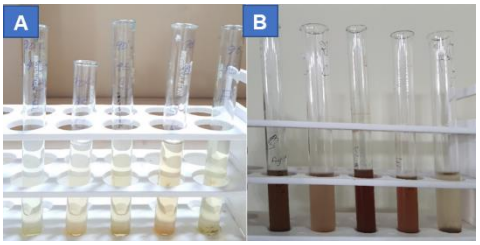

Figure 7 - Color change A) before 24 hours, B) after 24 hours.

The presence of AgNPs was indicated and confirmed by a well-distinctive peak in the visible range at 420 nm and 440 nm for samples A.muricata, A.squamosa green and A.squamosa red.

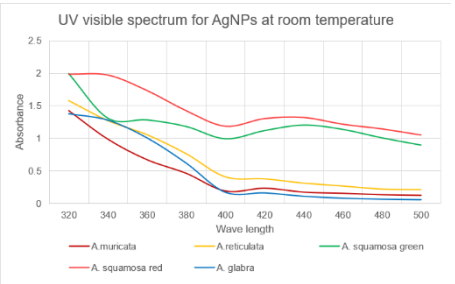

Figure 8 - UV visible spectrum for AgNPs at room temperature after 24 hours

Optimization table

Room temperature was considered the optimum temperature as three out of five samples produced AgNPs after 24 hours.

Table 4 - Optimization table

Sample	60°C				90°C				Room Temperature
	15 min	30 min	45 min	60 min	15 min	30 min	45 min	60 min	24 hours
A. muricata	X	X	X	X	X	X	X	X	✓
A. reticulata	X	X	X	X	X	X	X	X	X
A. squamosa Green	✓	✓	✓	✓	✓	✓	✓	✓	✓
A. squamosa Red	X	X	✓	X	X	✓	X	X	✓
A. glabra	X	X	X	✓	X	X	X	X	X

Scanning Electron Microscope

SEM images for A.squamosa red-AgNPs were obtained under different magnifications.

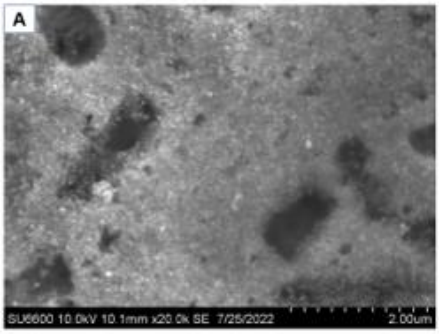

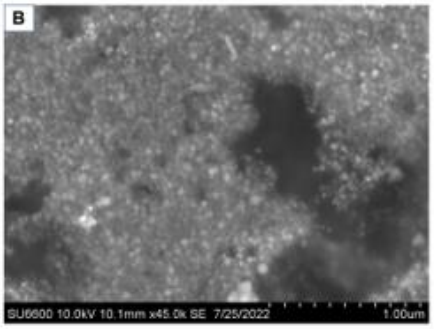

Figure 9 - SEM images under A) 20.0k B) 45.0k

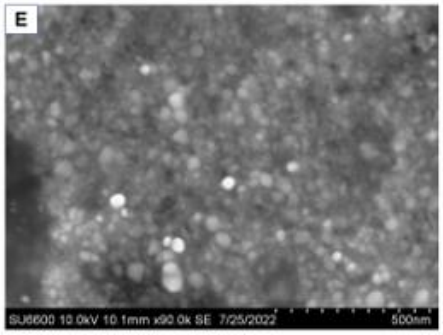

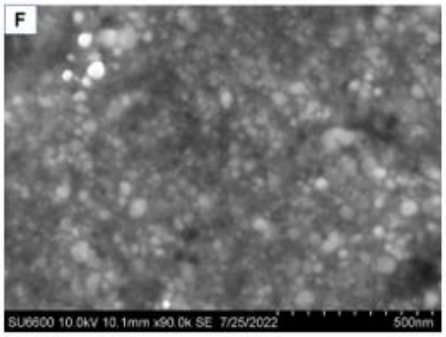

Figure 11 - SEM images under E) 90.0k F) 90.0k

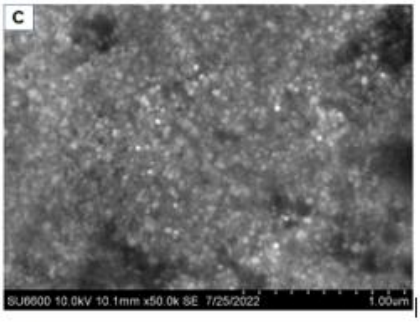

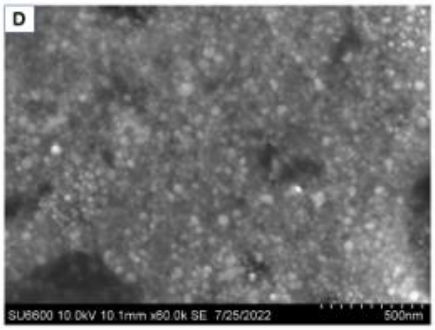

Figure 10 - SEM images under C) 50.0k D) 60.0k

The approximate particle size and shape of A.squamosa red is 40nm and spherical in shape.

Total Flavonoid Content

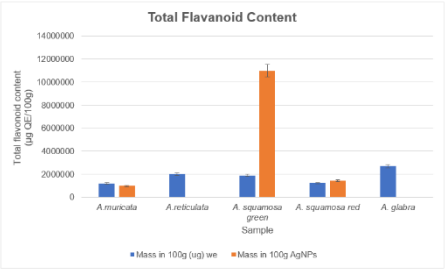

The TFC for the plant extract was greater than the AgNPs.

Table 5 - ANOVA table for TFC

ANOVA: Single Factor						
SUMMARY						
Groups	*Count*	*Sum*	*Average*	*Variance*		
Column 1	5	9026041.667	1805208.333	3.90698E+11		
Column 2	3	13390625	4463541.667	3.18914E+13		
ANOVA						
Source of Variation	*SS*	*df*	*MS*	*F*	*P-value*	*F crit*
Between Groups	1.32501E+13	1	1.32501E+13	1.216621982	0.312288	5.987378
Within Groups	6.53455E+13	6	1.08909E+13			
Total	7.85956E+13	7				

A significant difference was not observed as P> 0.05 (P = 0.312288).

Total Phenolic Content

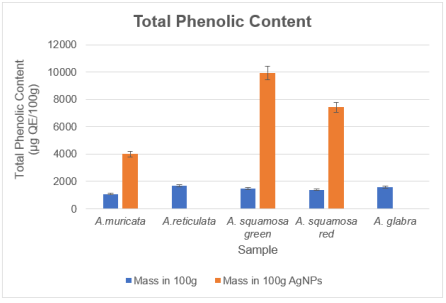

Figure 13 - The Total Phenolic Content.

The TPC for the AgNPs is greater than the water extract.

Table 6 - ANOVA table for TPC

ANOVA: Single Factor						
SUMMARY						
Groups	*Count*	*Sum*	*Average*	*Variance*		
Column 1	5	7183.214	1436.643	52075.09		
Column 2	3	21375.71	7125.238	8941548		
ANOVA						
Source of Variation	*SS*	*df*	*MS*	*F*	*P-value*	*F crit*
Between Groups	60675217.09	1	60675217	20.1229	0.004166	5.987378
Within Groups	18091395.6	6	3015233			
Total	78766612.69	7				

A significant difference was observed as P<0.05, (P= 0.004166).

Total Antioxidant Content.

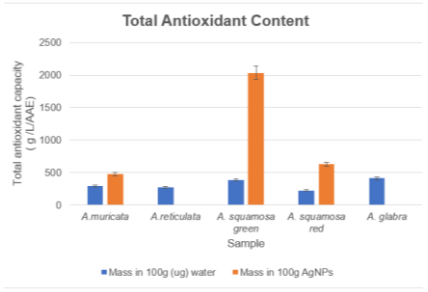

Figure 14 - The Total Antioxidant Content.

A greater TAC is observed in A.squamosa green-AgNPs.

Table 7 - ANOVA table for TAC

ANOVA: Single Factor						
SUMMARY						
Groups	*Count*	*Sum*	*Average*	*Variance*		
Column 1	5	1582.216	316.4432	5964.57		
Column 2	3	3136.25	1045.417	741271.1		
ANOVA						
Source of Variation	*SS*	*df*	*MS*	*F*	*P-value*	*F crit*
Between Groups	996379.3905	1	996379.4	3.968584	0.09344	5.987378
Within Groups	1506400.463	6	251066.7			
Total	2502779.854	7				

A significant difference was not observed as P > 0.05 (P=0.09344).

DPPH Assay

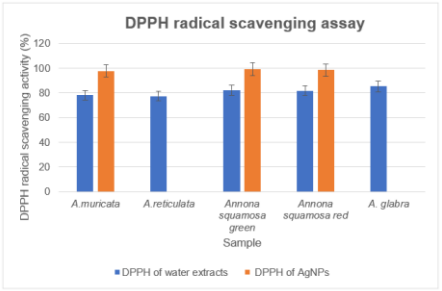

Figure 15 - DPPH radical scavenging activity.

DPPH radical scavenging activity was higher in all AgNPs.

Mean Inhibition Concentration (IC50).

Lower IC50 values were observed in AgNPs than water extract.

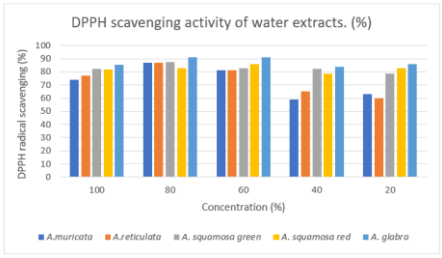

Figure 16 - IC50 for water extracts

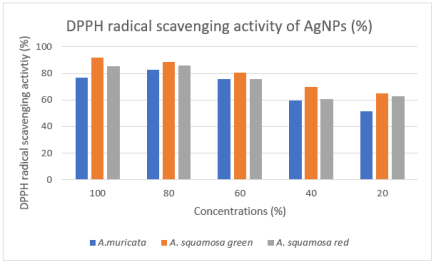

Figure 17 - IC50 for AgNPs.

Table 8 - IC50 of samples

Sample	Water Extract	AgNPs
Annona muricata	202.6753141	137.2118551
Annona reticulata	179.0830946	-
Annona squamosa green	823.723229	138.121547
Annona squamosa red	4761.904762	142.9796969
Annona glabra	1592.356688	-

Photocatalytic Activity.

The photocatalytic properties were evaluated by A.squamosa red under different conditions and concentrations.

Under Sunlight

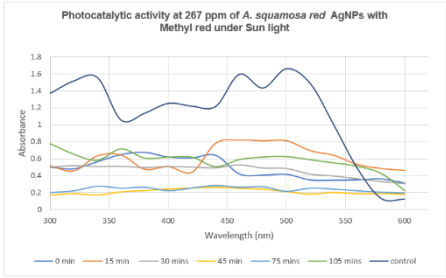

Figure 18 - Photocatalytic activity under sunlight at 267 ppm.

The MR dye was degraded by 45 minutes.

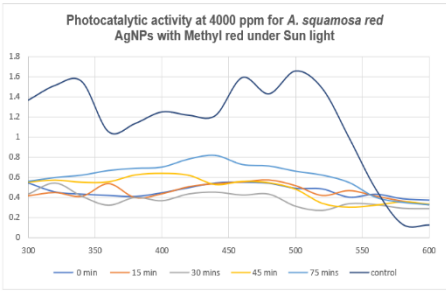

Figure 19 - Photocatalytic activity under sunlight at 4000 ppm.

The MR dye was degraded by 30 minutes under sunlight at 4000 ppm.

Under sunlight with NaBH4

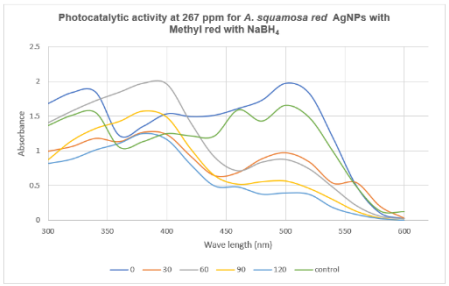

Figure 20 - Photocatalytic activity with catalyst at 267 ppm.

The dye was degraded by 120 minutes.

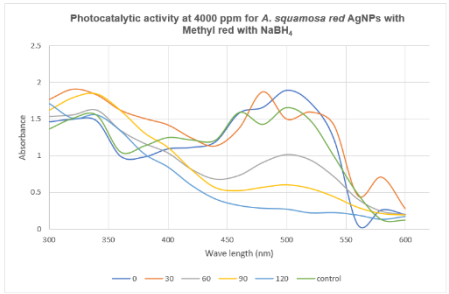

Figure 21 - Photocatalytic activity with catalyst at 4000 ppm.

The dye was degraded by 120 minutes.

A color change was observed in the presence of a catalyst under sunlight

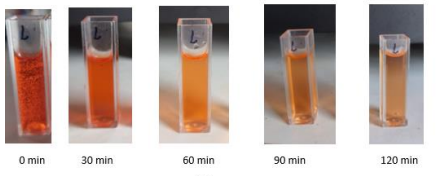

(a)

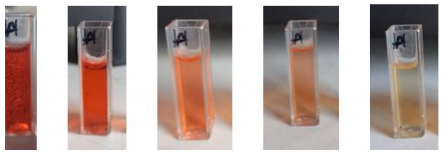

(b)

Figure 22 - Decolorization of MR for A.squamosa red: (a) 267 ppm (b) 4000 ppm.

A color change was observed in the presence of a catalyst under sunlight.

Antimicrobial Activity

The antimicrobial activity was observed by S. aureus. The ZOI of AgNPs was greater than the water extraction.

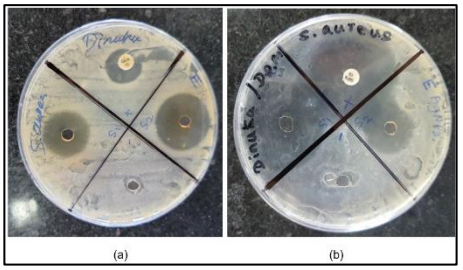

Figure 23 - Antimicrobial activity of A.squamosa red (a) leaf extracts and (b)AgNPs against S.aureus.

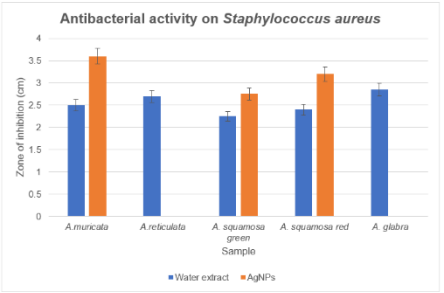

Figure 24 - Antimicrobial activity of water extracts and AgNPs against S.aureus.

A higher ZOI was observed in AgNPs than in water extracts.

Table 9 - ANOVA table for S.aureus.

ANOVA: Single Factor						
SUMMARY						
Groups	*Count*	*Sum*	*Average*	*Variance*		
Column 1	5	12.7	2.54	0.05675		
Column 2	3	9.55	3.183333	0.180833		
ANOVA						
Source of Variation	*SS*	*df*	*MS*	*F*	*P-value*	*F crit*
Between Groups	0.776020833	1	0.776021	7.909612	0.030659	5.987378
Within Groups	0.588666667	6	0.098111			
Total	1.3646875	7				

A significant difference was observed between water extract and AgNPs as P-value < 0.05 (P=0.030659).

The antimicrobial activity was observed by E.coli. The ZOI of AgNPs was greater than the water extraction.

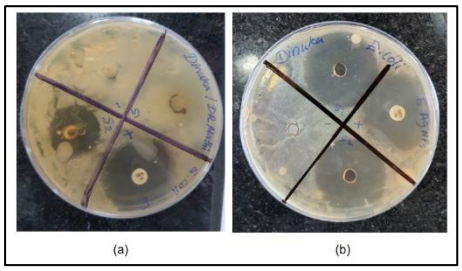

Figure 25 - Antimicrobial activity for A.squamosa red (a) the leaf extracts and (b) AgNPs against E.coli.

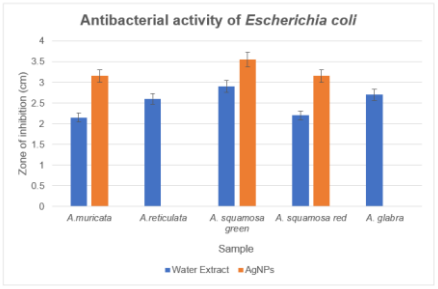

Figure 26 - Antibacterial activity of water extracts and AgNPs against E.coli.

A higher ZOI was observed in AgNPs than in water extracts.

Table 10 - ANOVA table for E.coli.

ANOVA: Single Factor						
SUMMARY						
Groups	*Count*	*Sum*	*Average*	*Variance*		
Column 1	5	12.55	2.51	0.1055		
Column 2	3	9.85	3.283333	0.053333		
ANOVA						
Source of Variation	*SS*	*df*	*MS*	*F*	*P-value*	*F crit*
Between Groups	1.121333333	1	1.121333	12.72636	0.011821	5.987378
Within Groups	0.528666667	6	0.088111			
Total	1.65	7				

A significant difference was observed between water extract and AgNPs as P < 0.05, (P=0.011821).

Table 11 - ANOVA table for both E.coli and S.aureus.

ANOVA: Single Factor						
SUMMARY						
Groups	*Count*	*Sum*	*Average*	*Variance*		
Column 1	8	22.25	2.78125	0.194955		
Column 2	8	22.4	2.8	0.235714		
ANOVA						
Source of Variation	*SS*	*df*	*MS*	*F*	*P-value*	*F crit*
Between Groups	0.001406	1	0.001406	0.006531	0.936736	4.60011
Within Groups	3.014688	14	0.215335			
Total	3.016094	15				

A significant difference was not observed as P> 0.05 (P=0.936736).

DISCUSSION

The selection of an environmentally friendly solvent like water, a suitable non-toxic reducing agent, and a safe chemical for stabilization are the three most crucial conditions for the green synthesis of AgNPs. (Hano & Abbasi, 2021). Phytochemicals play a crucial role in the formation of AgNPs as they act as a reducing agent converting Ag+1 ions to Ag0 and a capping agent therefore converting metal salts into metal nanoparticles. The development of AgNPs was first detected through a color change from a light-yellow solution to a dark red color after 24 hours, indicating a greater concentration of AgNPs. The formation of clusters of AgNPs was confirmed by the UV-Spectrophotometer as it indicated a distinctive peak between 420 nm – 440 nm. The peak and the change in color are observed due to the excitation of surface plasmons present on the outer surface of AgNPs occurs due to the presence of light/UV incident. The physical, chemical, and optical properties are determined by the surface plasmons (Malik et al., 2022).

The standard method to synthesize AgNPs was carried out prior to the optimized method at 90°C, and 60°C for 15,30, and 45 minutes respectively. Even

though a color change was observed, the heating approach was unsuccessful as there were no absorption peaks observed in the UV-spectrophotometer as phytochemicals may have been destroyed at higher temperatures.

The SEM images of A.squamosa red-AgNPs under different magnifications displayed that the particles are small spherical in shape with an approximate size of 40 nm. A study done by Malik et al., (2022) describes the larger size and agglomeration of the AgNPs caused by factors such as temperature showing a greater surface energy. The differential energy between the upper valence band and the lower band of the conductance band can leap from one band to another, this phenomenon is known as the band gap. The specific minimum energy needed for the transition for an electron is known as the band energy (Sundeep et al., 2017). To investigate the conductivity of the synthesized AgNPs (Table 12), Einstein's Photon Energy relation equation below was used to calculate the band gap energy. h = 6.626 × 10 -34 J s (Plank constant), C = 3 ×108 m/s (speed of light), and λ = cut-off wavelength for AgNPs.

$$E = \frac{hc}{\lambda max} \quad \text{Equation 2}$$

Table 12 - Electrical Conductance of AgNPs.

AgNPs Sample	Band Gap Energy	Category
Annona muricata	2.95 eV	Semiconductor
Annona squamosa green	2.82 eV	Semiconductor
Annona squamosa red	2.82 eV	Semiconductor

The AgNPs were categorized as semiconductors based on the calculated bandgap energies therefore can act as a photocatalyst. Smaller particles with few atoms have a greater conductance band energy due to the attraction between the metal ions and conductance electrons (Shrestha & Adhikari, 2017).

A colorimetric assay utilizing AlCl3 technique was performed to detect the TFC. AlCl3 produces acid-stable compounds with flavone and flavanols with C-3 or C-5 hydroxyl groups and C-4 keto groups (Figure 29) (Tristantini & Amalia, 2019).

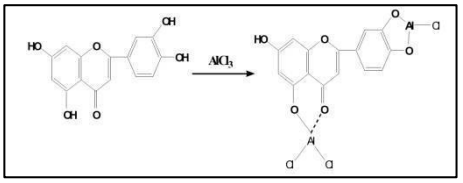

Figure 27 - Formation of flavonoid AlCl3 Complex (Makuasa & Ningsih, 2020).

A greater amount of TFC was observed in AgNPs than water extract (Figure 10) A.squamosa green-AgNPs >A.squamosa red-AgNPs > A.muricata-AgNPs. A significance difference between the water extract and AgNPs was not observed as P = 0.312288 (P > 0.05). Literature has revealed that various extracts of A.squamosa leaf extracts contain flavonoids (Nguyen et al., 2020).

The Folin-Ciocalteu test is based on the reduction of phenolic antioxidants which acts as a free radical terminator. Phosphotungstic acid/phosphomolybdic acid reduces to creates a blue chromophore and can be observed at a with a maximum wavelength of 765 nm. The central molybdenum ion acts as a reducing site by obtaining an electron from the phenolic compounds causing the reduction of Mo^{6+} to Mo^{5+} (Figure 30) (Munteanu & Apetrei, 2021).

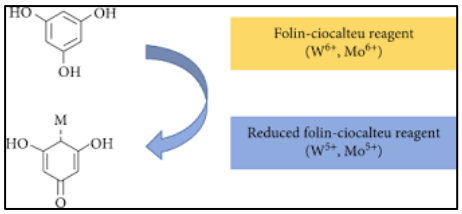

Figure 28 - Reduction of the FC reagent. (Ford et al., 2019).

A.squamosa green-AgNPs >A.squamosa red-AgNPs > A.muricata-AgNPs showed a greater TPC than the water extract (Figure 11). The One-way ANOVA table showed a statistical significance difference between the water extract and AgNPs was observed as P = 0.004166 (P < 0.05). Phenolic compounds aid in the formation and stabilization of AgNPs by acting as a capping agent and as a reducing molecule for silver ions. A previous study done on water extract of A.squamosa leaves has shown a greater amount of phenolic compounds on different parts of the plant (Nguyen et al., 2020).

The phosphomolybdenum assay evaluates the ability of the antioxidant to reduce Mo(VI) to Mo (V) and resulting in the development of a green-colored phosphomolybdenum V complex (Figure 31), which shows a maximum absorbance at 695 nm (Fowsiya & Madhumitha, 2017).

Figure 29 - TAC Mechanism of Action (Fowsiya & Madhumitha, 2017).

Higher TAC was observed in AgNPs than in water extracts (Figure 12). A.squamosa green-AgNPs >A.squamosa red-AgNPs > A.muricata-AgNPs showed a greater TPC than the water extract. One-way ANOVA table was performed. There was no significance difference between the water extract and AgNPs as P = 0.09344 (P > 0.05). A previous study performed on A.squamosa water leaves extract have showed the presence of antioxidant compounds (El-Chaghaby, Ahmad & Ramis, 2014).

The DPPH assay measures the antioxidants capacity to reduce the DPPH radical. The organic nitrogen radical is neutralized from the antioxidant species by either taking a hydrogen atom or an electron (Figure 32). Thus, changing the initial purple color to a yellow color. The 30 minutes incubation enables DPPH to react effectively even in the presence of weak antioxidants (Bibi Sadeer et al., 2020). All AgNPs samples obtained a greater DPPH scavenging activity than the water extract (Figure 13). A previous study done on A.muricata AgNPs leaves revealed a strong action against DPPH (Badmus et al., 2020).

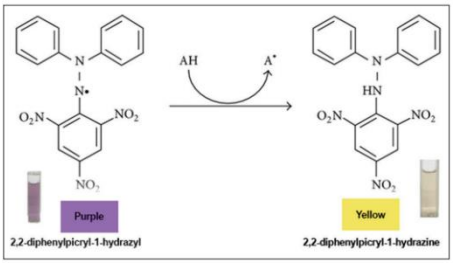

Figure 30 - Neutralization of DPPH radical (Marjoni, 2018)

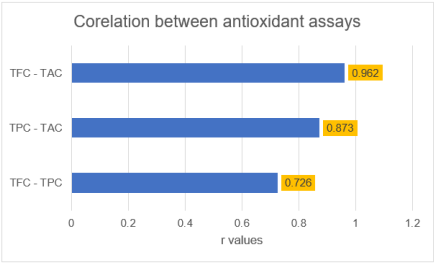

Figure 31 - Correlation between antioxidant assays

Pearson correlation factor (Figure 33) showed a strong correlation between TFC – TAC (r= 0.962), and TPC – TAC (r=0.873). While a moderate correlation was observed between TFC – TPC (r=0.726). This implies that the antioxidant activity and the antioxidant content are directly proportional to each assay. A study done on A.muricata shows a strong positive correlation between TPC-TAC, TFC-TAC. (Du et al., 2021).

Results obtained from the DPPH radical scavenging assays can be displayed in a number of different ways, such as the IC50. The number of antioxidants required to reduce the initial DPPH concentration by 50% is known as the IC50 value. (Martinez-Morales et al., 2020). The values obtained for IC50 AgNPs were lower than the water extracts indicating a higher antioxidant capacity (Table 8). Since IC50 values are inversely related to antioxidant activity, a low IC50 value represents a stronger ability of the sample to act as a DPPH scavenger. The lower IC50 value is due to the presence of a higher content of TFC and TPC clearly seen from the Pearson correlation (Figure 33). The action of AgNPs is more prominent in E.coli than S.aureus due to the thicker cell walls of gram-positive bacteria which causes the penetration of Ag+ into the cytoplasm. Electrostatic interactions between the Ag+ ions and the negatively charged lipopolysaccharide cell wall surface causes the AgNPs to adhere to the gram-negative bacterial cell wall, increasing the permeability to increase leading to structural changes in the cell membrane (Figure 34). Cellular toxicity caused by ROS, puts cells under oxidative stress which leads to the disruption of signal transduction pathways (Mikhailova, 2020).

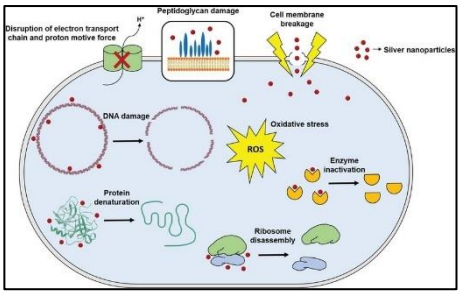

Figure 32 - Antibacterial action due to AgNPs (Roy et al., 2019).

A higher ZOI was seen in AgNPs than the water extracts for both bacteria. (Figure 24 and 26) E.coli showed a greater ZOI for AgNPs than S.aureus. One-way ANOVA results indicated the significant difference between the antimicrobial activity of water extracts and AgNPs against S.aureus as the P value < 0.05 (P=0.03066). E.coli showed a significance difference as P value < 0.05 (P=0.01182). Nevertheless, a significant difference was not observed between the action of the two bacteria. A previous study done on A.reticulata-AgNPs leaves depicted the antibacterial action for S.aureus and E.coli with a smaller ZOI (Parthiban et al., 2019).

The photocatalytic activity was carried for two different concentrations of A.squamosa red-AgNPs (264 ppm and 4000 ppm) using MR in the presence of UV, sunlight and NaBH4 catalyst in the presence of sunlight (Figure 35).

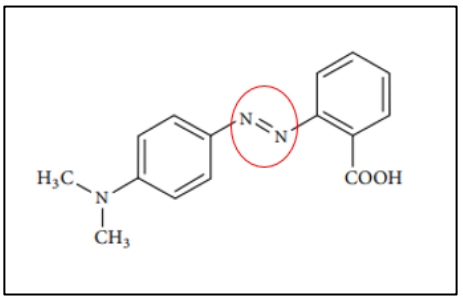

Figure 33 - Structure of MR (Ebrahimi and Modrek, 2013).

In response to the absorption of sunlight by the AgNPs, the SPR effect causes an electron from the outer band to get stimulated to a higher energy state. The dye molecule is attacked and degraded by the excited electrons as they react with oxygen molecules to create O2• and the hydroxyl ion •OH (Figure 36). The large surface area of the AgNPs absorbs the dye molecules without impairing their function. MR is degraded as the dye molecules are being taken up by the electron holes created in the AgNPs (Hermosilla et al., 2022).

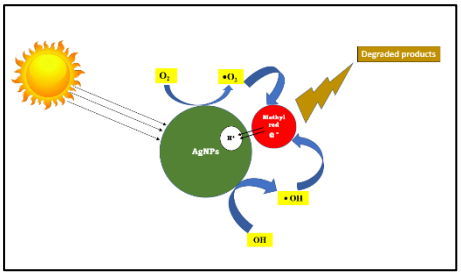

Figure 34 - Photocatalytic degradation of methyl red by AgNPs.

The dye was degraded by sunlight, UV, and sunlight in the presence of NaBH4 for all concentrations. The dye is degraded by AgNPs using an electron transfer mechanism in the presence of NaBH4. As a result of the [BH4-] ions are adhering on the surface of AgNPs results in an electron transfer from [BH4] ions to the dye through the nanoparticles, causing the MR chromophore to be destroyed (Figure 37) (Mathew, 2018).

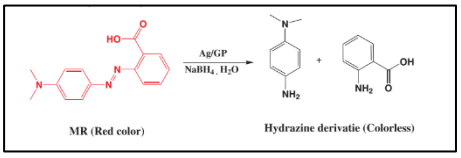

Figure 35 - Mechanism of action of MR with NaBH4 (Ismail et al., 2019).

The intensity of the peak gradually decreased over time indicating a deprotonation of MR indicating the breakdown of the azo site resulting in the production of aromatic amines with lower molecular weight (Ismail et al., 2019).

The rate kinetics of the photocatalytic degradation of MR was calculated by pseudo-first order rate law, by the following equation 3, and the values are given in table 13.

$$\ln \frac{c}{c_0} = kt \qquad \text{Equation 3}$$

C = MR concentration, C0 = Initial MR concentration, k = Rate constant and t = time

Table 13 - Rate constant for different concentrations and conditions.

Condition	K Value	
	267 ppm	4000 ppm
UV	0.7986	0.0439
Sunlight	0.21	0.7341
Sunlight and $NaBH_4$	0.9244	0.952

The rate constant was calculated from the gradient of equation 2 (Figure 38 and 39). In comparison to 267 ppm a higher rate constant was obtained at 4000 ppm under sunlight with NaBH4. Therefore, has been proposed to have an effective photocatalytic degradation capacity.

Research done on A.squamosa-AgNPs seed extract has proven the photocatalytic degradation of Coomassie Brilliant Blue within 30 minutes (Jose et al., 2021).

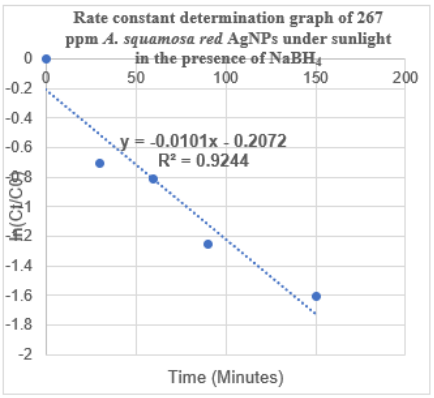

Figure 36 - Rate constant graph of 267 ppm

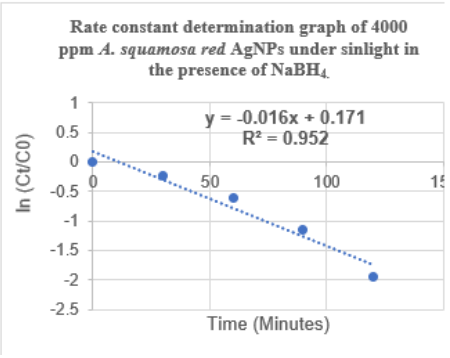

Figure 37 - Rate constant graph of 4000 ppm.

In conclusion the green synthesis of AgNPs from three out of five varieties of Annonaceae leaf extracts was successful. The optimum temperature was at room temperature at 24 hours. The AgNPs showed a greater antioxidant content than the water extracts. A significant difference was observed in the zone of inhibition between the water extract and the AgNPs for E.coli and S.aureus. The photocatalytic activity of A.squamosa red-AgNPs was found to be more efficient for the photocatalytic degradation of methyl red in 120 minutes than 3000 ppm for A.squamosa red-AgNPs under the sunlight with NaBH4. Therefore, due to these properties AgNPs can be utilized as a therapeutic agent.

Future work

- As of future work extraction of Annona leaves for the green synthesis of AgNPs can be performed under several types of polar solvents ethanol or methanol, and non-polar solvents such as hexane, benzene thereby can be used to extract polar active compounds and non-polar active compounds. The findings can be further extended using different parts of the Annona plant such as roots, bark, seeds.
- To observe a higher resolution and better morphology further analysis of the AgNPs could be performed by transmission electron microscope and atomic force microscope, X-ray diffraction analysis and energy dispersive spectroscopy.
- To analysis antioxidant properties, assays such as Oxygen Radical Absorbance Capacity, Ferric Reducing Antioxidant Power Assay can be performed on the samples.
- The photocatalytic activity of the AgNPs can be further tested with different dyes such as methyl orange, eriochrome black T, methyl blue, malachite green. It can then be further analyzed to degenerate toxic products from polluted waterways.
- Antibacterial testing can be performed on different types of gram positive and gram negative bacteria such as vibrio cholerae, salmonella, Staphylococcus epidermidis, Vibrio vulnificus, Campylobacter jejuni, and fungus types such as Aspergillus fumigates. Due to the insecticide ability of Annona plants this can be tested to naturally control insects such as larvae or mosquitos in Sri Lanka.
- As Annona plants have anticancer properties further analysis can be performed on different cancer cell lines for all water extracts and the synthesized AgNPs.

REFERENCES

Badmus, J.A., Oyemomi, S.A., Adedosu, O.T., Yekeen, T.A., Azeez, M.A., Adebayo, E.A., Lateef, A., Badeggi, U.M., Botha, S., Hussein, A.A. and Marnewick, J.L. (2020) 'Photo-assisted bio-fabrication of silver nanoparticles using Annona muricata leaf extract: exploring the antioxidant, anti-diabetic, antimicrobial, and cytotoxic activities', Heliyon, 6(11), p. e05413. doi:10.1016/j.heliyon.2020.e05413.

Baig, N., Kammakakam, I. and Falath, W. (2021) 'Nanomaterials: a review of synthesis methods, properties, recent progress, and challenges', Materials Advances, 2(6), pp. 1821–1871. doi:10.1039/d0ma00807a.

Bibi Sadeer, N., Montesano, D., Albrizio, S., Zengin, G. and Mahomoodally, M.F. (2020) 'The Versatility of Antioxidant Assays in Food Science and Safety—Chemistry, Applications, Strengths, and Limitations', Antioxidants, 9(8), p. 709. doi:10.3390/antiox9080709.

Coria-Téllez, A.V., Montalvo-Gónzalez, E., Yahia, E.M. and Obledo-Vázquez, E.N. (2018) 'Annona muricata: A comprehensive review on its traditional medicinal uses, phytochemicals, pharmacological activities, mechanisms of action and toxicity', Arabian Journal of Chemistry, 11(5), pp. 662–691. doi:10.1016/j.arabjc.2016.01.004.

Dhand, C., Dwivedi, N., Loh, X.J., Jie Ying, A.N., Verma, N.K., Beuerman, R.W., Lakshminarayanan, R. and Ramakrishna, S. (2015) 'Methods and strategies for the synthesis of diverse nanoparticles and their applications: a comprehensive overview', RSC Advances, 5(127), pp. 105003–105037. doi:10.1039/c5ra19388e.

Du, J., Zhong, B., Subbiah, V., Barrow, C.J., Dunshea, F.R. and Suleria, H.A.R. (2021) 'LC-ESI-QTOF-MS/MS Profiling and Antioxidant Activity of Phenolics from Custard Apple Fruit and By-Products', Separations, 8(5), p. 62. doi:10.3390/separations8050062.

Ebrahimi, H.R. and Modrek, M. (2013) 'Photocatalytic Decomposition of Methyl Red Dye by Using Nanosized Zinc Oxide Deposited on Glass Beads in Various pH and Various Atmosphere', Journal of Chemistry, 2013, p. e151034. doi:10.1155/2013/151034.

El-Chaghaby, G.A., Ahmad, A.F. and Ramis, E.S. (2014) 'Evaluation of the antioxidant and antibacterial properties of various solvents extracts of Annona squamosa L. leaves', Arabian Journal of Chemistry, 7(2), pp. 227–233. doi:10.1016/j.arabjc.2011.06.019.

Fanoro, O.T. and Oluwafemi, O.S. (2020) 'Bactericidal Antibacterial Mechanism of Plant Synthesized Silver, Gold and Bimetallic Nanoparticles', Pharmaceutics, 12(11), p. 1044. doi:10.3390/pharmaceutics12111044.

Ford, L., Theodoridou, K., Sheldrake, G.N. and Walsh, P.J. (2019) 'A critical review of analytical methods used for the chemical characterisation and quantification of phlorotannin compounds in brown seaweeds', Phytochemical Analysis, 30(6), pp. 587–599. doi:10.1002/pca.2851.

Fowsiya, J. and Madhumitha, G. (2017) 'Preliminary phytochemical analysis, Antioxidant and cytotoxicity test ofCarissa edulisVahl dried fruits', IOP Conference Series: Materials Science and Engineering, 263, p. 022018. doi:10.1088/1757-899x/263/2/022018.

Hano, C. and Abbasi, B.H. (2021) 'Plant-Based Green Synthesis of Nanoparticles: Production, Characterization and Applications', Biomolecules, 12(1), p. 31. doi:10.3390/biom12010031.

Hemlata, Meena, P.R., Singh, A.P. and Tejavath, K.K. (2020) 'Biosynthesis of Silver Nanoparticles Using Cucumis prophetarum Aqueous Leaf Extract and Their Antibacterial and Antiproliferative Activity Against

Cancer Cell Lines', ACS Omega, 5(10), pp. 5520–5528. doi:10.1021/acsomega.0c00155.

Hermosilla, E., Díaz, M., Vera, J., Seabra, A.B., Tortella, G., Parada, J. and Rubilar, O. (2022) 'Molecular Weight Identification of Compounds Involved in the Fungal Synthesis of AgNPs: Effect on Antimicrobial and Photocatalytic Activity', Antibiotics, 11(5), p. 622. doi:10.3390/antibiotics11050622.

Hood, E. (2004) 'Nanotechnology: Looking As We Leap', Environmental Health Perspectives, 112(13), pp. A740–A749.

Ismail, M., Khan, M.I., Khan, M.A., Akhtar, K., Asiri, A.M. and Khan, S.B. (2019) 'Plant-supported silver nanoparticles: Efficient, economically viable and easily recoverable catalyst for the reduction of organic pollutants', Applied Organometallic Chemistry, 33(8). doi:10.1002/aoc.4971.

Jagtap, U.B. and Bapat, V.A. (2012) 'Antioxidant activities of various solvent extracts of custard apple (Annona squamosa L.) fruit pulp', Nutrafoods, 11(4), pp. 137–144. doi:10.1007/s13749-012-0053-8.

Jose, V., Raphel, L., Aiswariya, K.S. and Mathew, P. (2021) 'Green synthesis of silver nanoparticles using Annona squamosa L. seed extract: characterization, photocatalytic and biological activity assay', Bioprocess and Biosystems Engineering [Preprint]. doi:10.1007/s00449-021-02562-2.

Kandiah, M. and Perera, B.R. (2018) 'Microwave Assisted One-Pot Green Synthesis of Silver Nanoparticles Using Leaf Extracts from Vigna Unguiculate: Evaluation of Antioxidant and Antimicrobial Activities', International Journal of Multidisciplinary Studies, 5(2). doi:10.31357/ijms.v5i2.3968.

Kumar, T. and Jain, V. (2015) 'Appraisal of Total Phenol, Flavonoid Contents, and Antioxidant Potential of FolkloricLannea coromandelicaUsingIn VitroandIn VivoAssays', Scientifica, 2015, pp. 1–13. doi:10.1155/2015/203679.

Lee, S.H. and Jun, B.-H. (2019) 'Silver Nanoparticles: Synthesis and Application for Nanomedicine', International journal of molecular sciences, 20(4), p. 865. doi:10.3390/ijms20040865.

Lorigo, M. and Cairrao, E. (2019) 'Antioxidants as stabilizers of UV filters: an example for the UV-B filter octylmethoxycinnamate', Biomedical Dermatology, 3(1). doi:10.1186/s41702-019-0048-9.

Lourenço, S.C., Moldão-Martins, M. and Alves, V.D. (2019) 'Antioxidants of Natural Plant Origins: From Sources to Food Industry Applications', Molecules, 24(22), p. 4132. doi:10.3390/molecules24224132.

Makuasa, D.A.A. and Ningsih, P. (2020) 'The Analysis of Total Flavonoid Levels In Young Leaves and Old Soursop Leaves (Annona muricata L.) Using UV-Vis Sepctrofotometry Methods', Journal of Applied Science, Engineering, Technology, and Education, 2(1), pp. 11–17. doi:10.35877/454RI.asci2133.

Malik, M., Iqbal, M.A., Malik, M., Raza, M.A., Shahid, W., Choi, J.R. and Pham, P.V. (2022) 'Biosynthesis and Characterizations of Silver Nanoparticles from Annona squamosa Leaf and Fruit Extracts for Size-Dependent Biomedical Applications', Nanomaterials, 12(4), p. 616. doi:10.3390/nano12040616.

Marjoni, M.R. (2018) 'Extraction of antioxidants from fruit peel of Artocarpus altilis', International Journal of Green Pharmacy (IJGP), 12(01). doi:10.22377/ijgp.v12i01.1635.

Martinez-Morales, F., Alonso-Castro, A.J., Zapata-Morales, J.R., Carranza-Álvarez, C. and Aragon-Martinez, O.H. (2020) 'Use of standardized units for a correct interpretation of IC50 values obtained from the inhibition of the DPPH radical by natural antioxidants', Chemical

Papers, 74(10), pp. 3325–3334. doi:10.1007/s11696-020-01161-x.

Mathew, B. (2018) 'Treatment of Water Effluents Using Silver Nanoparticles', Material Science & Engineering International Journal, 2(5). doi:10.15406/mseij.2018.02.00050.

Melkamu, W.W. and Bitew, L.T. (2021) 'Green synthesis of silver nanoparticles using Hagenia abyssinica (Bruce) J.F. Gmel plant leaf extract and their antibacterial and anti-oxidant activities', Heliyon, p. e08459. doi:10.1016/j.heliyon.2021.e08459.

Mikhailova, E.O. (2020) 'Silver Nanoparticles: Mechanism of Action and Probable Bio-Application', Journal of Functional Biomaterials, 11(4), p. 84. doi:10.3390/jfb11040084.

Munteanu, I.G. and Apetrei, C. (2021) 'Analytical Methods Used in Determining Antioxidant Activity: A Review', International Journal of Molecular Sciences, 22(7), p. 3380. doi:10.3390/ijms22073380.

Mustapha, T., Misni, N., Ithnin, N.R., Daskum, A.M. and Unyah, N.Z. (2022) 'A Review on Plants and Microorganisms Mediated Synthesis of Silver Nanoparticles, Role of Plants Metabolites and Applications', International Journal of Environmental Research and Public Health, 19(2), p. 674. doi:10.3390/ijerph19020674.

Nguyen, M.T., Nguyen, V.T., Le, V.M., Trieu, L.H., Lam, T.D., Bui, L.M., Nhan, L.T.H. and Danh, V.T. (2020) 'Assessment of preliminary phytochemical screening, polyphenol content, flavonoid content, and antioxidant activity of custard apple leaves (Annona squamosa Linn.)', IOP Conference Series: Materials Science and Engineering, 736, p. 062012. doi:10.1088/1757-899x/736/6/062012.

Parthiban, E., Manivannan, N., Ramanibai, R. and Mathivanan, N. (2019) 'Green synthesis of silver-nanoparticles from Annona reticulata leaves aqueous extract and its mosquito larvicidal and anti-microbial activity on human pathogens', Biotechnology Reports, 21, p. e00297. doi:10.1016/j.btre.2018.e00297.

Roy, A., Bulut, O., Some, S., Mandal, A.K. and Yilmaz, M.D. (2019) 'Green synthesis of silver nanoparticles: biomolecule-nanoparticle organizations targeting antimicrobial activity', RSC Advances, 9(5), pp. 2673–2702. doi:10.1039/c8ra08982e.

Roy, K., Sarkar, C.K. and Ghosh, C.K. (2015) 'Photocatalytic activity of biogenic silver nanoparticles synthesized using potato (Solanum tuberosum) infusion', Spectrochimica Acta Part A: Molecular and Biomolecular Spectroscopy, 146, pp. 286–291. doi:10.1016/j.saa.2015.02.058.

Selvaraj, V., Sagadevan, S., Muthukrishnan, L., Johan, Mohd.R. and Podder, J. (2019) 'Eco-friendly approach in synthesis of silver nanoparticles and evaluation of optical, surface morphological and antimicrobial properties', Journal of Nanostructure in Chemistry, 9(2), pp. 153–162. doi:10.1007/s40097-019-0306-9.

Shrestha, S. and Adhikari, S. (2017) 'Size Dependent Optical Properties of Silver Nanoparticles Synthesized from Fruit Extract of Malus pumila', Journal of Nepal Chemical Society, 37, pp. 43–48. doi:10.3126/jncs.v37i0.32111.

Singh, J., Dutta, T., Kim, K.-H., Rawat, M., Samddar, P. and Kumar, P. (2018) '"Green" synthesis of metals and their oxide nanoparticles: applications for environmental remediation', Journal of Nanobiotechnology, 16(1). doi:10.1186/s12951-018-0408-4.

Sreedharan, V. and Bhaskara Rao, K.V. (2019) 'Biodegradation of Textile Azo Dyes', Nanoscience and Biotechnology for Environmental Applications, pp. 115–139. doi:10.1007/978-3-319-97922-9_5.

Sundeep, D., Vijaya Kumar, T., Rao, P.S.S., Ravikumar, R.V.S.S.N. and Gopala

Krishna, A. (2017) 'Green synthesis and characterization of Ag nanoparticles from Mangifera indica leaves for dental restoration and antibacterial applications', Progress in Biomaterials, 6(1-2), pp. 57–66. doi:10.1007/s40204-017-0067-9.

Tristantini, D. and Amalia, R. (2019) 'Quercetin concentration and total flavonoid content of anti-atherosclerotic herbs using aluminum chloride colorimetric assay', AIP Conference Proceedings [Preprint]. doi:10.1063/1.5139349.

Valko, M., Leibfritz, D., Moncol, J., Cronin, M.T.D., Mazur, M. and Telser, J. (2007) 'Free radicals and antioxidants in normal physiological functions and human disease', The International Journal of Biochemistry & Cell Biology, 39(1), pp. 44–84. doi:10.1016/j.biocel.2006.07.001.

Vatandoostarani, S., Bagheri Lotfabad, T., Heidarinasab, A. and Yaghmaei, S. (2017) 'Degradation of azo dye methyl red by Saccharomyces cerevisiae ATCC 9763', International Biodeterioration & Biodegradation, 125, pp. 62–72. doi:10.1016/j.ibiod.2017.08.009.

Zhang, X.-F., Liu, Z.-G., Shen, W. and Gurunathan, S. (2016) 'Silver Nanoparticles: Synthesis, Characterization, Properties, Applications, and Therapeutic Approaches', International Journal of Molecular Sciences, 17(9), p. 1534. doi:10.3390/ijms17091534